Earthquake Engineering, Tenth World Conference © 1992 Balkema, Rotterdam. ISBN 90 5410 060 5

Dynamic behavior of embedded structure on hard rock site

Tomoyuki Inukai & Tamio Imazawa
Takenaka Corporation, Tokyo, Japan
Kaoru Kusakabe
Kobe University, Japan
Masashi Yamamoto
Nuclear Power Engineering Center, Tokyo, Japan

ABSTRACT: In order to investigate the embedment effects on dynamic soil-structure interaction, the forced vibration tests were carried out under conditions of different embedment depths at an actual hard rock site. These tests used a large scale test model designed in consideration of the fundamental dynamic characteristics of PWR-type reactor buildings constructed in Japan. In this study the embedment effects at hard rock sites were confirmed by the test results. Simulation analyses of the test results were carried out employing two analytical models, namely the sway-rocking model and the axisymmetric FEM model. These models were verified to be applicable to evaluate the embedment effects.

1 INTRODUCTION

The effects of dynamic soil-structure interaction play an important role on the dynamic behavior of high massive and stiff structures, that is a nuclear reactor building, during earthquakes. One of these effects is the embedment effects that are as follows; "increase of the soil spring constant", "increase of the radiational damping" and "variation of the effective input motion".

In order to investigate the embedment effect on the structure response, forced vibration tests were carried out under condition of different embedment depths. These tests used a large scale test model constructed on an actual hard rock site. In the simulational analyses of the test results, the following two analytical models were used: (1) sway-rocking model employing the dynamic soil impedances of the bottom determined by the three dimensional wave propagation theory in layered media and the side impedances determined by Novak's method, and (2) axisymmetric FEM model.

This paper describes the test results and the analytical results.

2 CONDITION OF THE FORCED VIBRATION TEST

2.1 Test model and soil condition

The forced vibration tests were carried out under conditions of different embedment depths, namely non-embedment case and full-embedment case referred as to Test D1 and Test D2 respectively as shown in Fig. 1. The large scale test model was designed in consideration of the fundamental dynamic characteristics, which are non-dimensional frequency and mode shapes, of the PWR-type reactor buildings constructed in Japan. The test model is a 2-story RC structure with shear walls in NS direction and an 8m square foundation as shown in Fig. 2. The height is 10m and the total weight is about 920tons.

The test model was constructed on an actual hard rock site after excavating the ground 5m below the surface. According to the boring survey and the PS logging, the shear wave velocity of the supporting ground is about 1000m/s and its structure is almost uniform. In the backfilling work after Test D1, the thickness of each layer for once was 15cm and the target shear wave velocity was about 130m/s (125-135m/s). Therefore, in Test D2, the impedance ratio between the backfill soil and the supporting ground is quite high.

2.2 Method of experiment

The forced vibration tests were carried out by applying the harmonic force generated by the exciter installed at the center of the top floor or the base mat floor, referred as to RF- or BF-excitation respectively. the excitation moment was properly set within 60-400kgf·cm so that the backfill soil and the surrounding ground remained in elastic range.

The steady-state responses to the harmonic excitation, the amplitude and the phase lag, were measured. The responses of the test model were measured by displacement transducers. The responses of the surrounding ground and the backfill soil were also measured by displacement transducers and accelerometers.

3 TEST RESULTS

3.1 Response of test model

Table 1 shows the vibration characteristics of the test model. The values were obtained from the horizontal components of the resonance curves at the top floor. The non-dimensional frequency a_0, in Test D1, is

$$a_0 = w_0 \cdot b/Vs = 0.55$$

where w_0: natural circular frequency of soil-structure interaction system
b : foundation width
Vs: shear wave velocity of supporting ground

Fig. 3 shows the comparison of Test D1 and Test D2 on the resonance curves at the center of the base bottom. For the embedment effects exerted upon the vibration behaviors of the test model supported on the hard ground, the followings can be clarified:

1) Due to the embedment effects, the responses of the test model to a unit force at the resonance frequency decrease to large extent.

2) In the embedded case, the radiational damping effect is added from the side of the test model so that the damping factor of the soil-structure interaction system increases.

3) Since the impedance ratio between the backfill soil (Vs=130m/s) and the supporting ground (Vs=1000m/s) is quite high, the dynamic characteristics of the soil-structure interaction system is controlled by the supporting ground condition.

4) Due to the high impedance ratio of the ground, the change of the natural frequency caused by the embedment effect, that is the binding effect of the backfill soil, is small.

5) In both tests, the ratio of the elastic deformation of the super-structure in the displacement at top floor is high and the change of the ratio caused by embedment is very small.

3.2 Dynamic soil impedance

Fig. 4 shows the comparison of the dynamic soil impedances between Test D1 and Test D2. In this study, the dynamic soil impedances, K_{HH} (horizontal impedance) and K_{RR} (rotational impedance) are converted from the test results of RF- and BF-excitation using the relation of equations (1-1, 2).

$$Q/u_0 = K_H = K_{HH} + K_{HR} \cdot \theta_0/u_0 \qquad (1\text{-}1)$$

$$M/\theta_0 = K_R = K_{RR} + K_{RH} \cdot u_0/\theta_0 \qquad (1\text{-}2)$$

where

u_0, θ_0 : horizontal and rotational displacement at foundation bottom
Q, M : shearing force and moment at foundation bottom
K_H, K_R : combined horizontal and rotational impedances
$K_{HR}=K_{RH}$: dynamic coupling soil impedance

From Fig. 4, the followings are clarified:

1) In the low frequency range, the real part of the impedances, which indicates soil stiffness, increases by the binding effect of the backfill soil.

2) In the frequency range which is higher than the natural frequency of the soil-structure interaction system, there are a few frequency ranges where the real part of the soil impedance obtained from Test D2, the full-embedment case, becomes rather small compared with Test D1, the non-embedment case.

3) The imaginary part of impedances, which indicates the radiational damping effect, increases due to the embedment effect. This tendency is outstanding in the frequency range higher than the natural frequency of the soil-structure interaction system.

4 SIMULATIONAL ANALYSES

4.1 Analytical models

The simulational analyses of the tests results are worked out in the case of full-embedment, Test D2. In this study, the embedded part of the test model is treated as a rigid body based on the test results. The super-structure is modeled as a two lumped mass model with flexural deformation. In order to evaluate dynamic soil impedances, the following two analytical models are used;

1) Sway-rocking model shown in Fig. 5, hereafter called the S-R model. The dynamic soil impedances K_{HH}, K_{RR} and K_{HR} at center of the base bottom and the impedances K_U, and $K\phi$ at the side wall of the embedded part are evaluated by different analytical techniques. Assuming that the base level is a flat ground surface, the frequency dependent soil impedances of the square foundation are determined using the three dimensional wave propagation theory in layered half space. The side impedances caused by the backfill soil and the surrounding ground is calculated by Novak's method assuming an circular foundation with equivalent area equal to the square foundation. the analytical model for Novak's method is shown in Fig. 6

2) Axisymmetric finite element method, hereafter called the FEM model. To account for the energy dissipation from the analytical boundary, the FEM model is equipped with a viscous damping boundary at the bottom boundary and a transmitting boundary at the side boundary. Fig. 7 shows the FEM model. In this model, the square foundation is

replaced by the circular foundation with equivalent area equal to the square foundation.

Table 2 shows the constants of the soil used in this simulational analyses. These values were decided based on the results of the PS logging, the boring examination and the exploration with elastic waves carried out in the site. The numbers in Fig. 6 and 7 correspond to the layer numbers in Table 2 respectively. In the S-R model, the shear wave velocity of the top layer under the base, of which thickness is 0.5m, is 420m/s.

4.2 Analytical results

Fig. 8 shows the comparison of the test and analytical results on the dynamic soil impedances, K_{HH} (horizontal component) and K_{RR} (rotational component). As shown in Fig. 8, both analytical results obtained by the S-R model and the FEM model correspond well to the test results. As for the horizontal impedance, the real part of the analytical results is overestimated in the lower frequency range. While in the higher range, the results by the FEM model shows better agreement with the test results than the results by the S-R model. As for the real part of rotational impedance, the analytical results are overestimated in the higher frequency range.

Fig. 9 shows the comparison of the test and analytical results on the resonance curves of displacement at the top of the test model. In the simulational analyses, the dynamic soil impedances K_{HH}, K_{HR} and K_{RR}, obtained as mentioned above, are used. The analytical results are in good agreement with the test results on both the amplitude and the phase lag. Therefore the analytical model of the test model and the soil condition are confirmed to be appropriate to the analyses. As for the amplitude near the resonance frequency, the result of the FEM model is overestimated, while the result of the S-R model is underestimated, but the differences between the test and analyses are very small.

Fig. 10 shows the comparison of the test result and the analytical result of the FEM model on the resonance curves of acceleration in the backfill soil and the surrounding soil. The analytical results are in good agreement with the test results, while the amplitude of the measuring points in the slope of the surrounding ground shows the discrepancy in the higher frequency range.

5 CONCLUSIONS

The concluding remarks obtained from the experimental and analytical studies on the embedment effect of dynamic soil-structure interaction are as follows:

1) The resonance response amplitude of the test model decreases by the embedment effect namely increase of radiational damping.

2) In this study, the binding effect of the backfill soil, that is the increase of the soil spring constant, is small because of the high impedance ratio between the backfill soil and the supporting ground. Therefore, the resonance frequency does not shift to so high frequency. And the dynamic behaviors of the soil-structure interaction system is controlled by supporting ground condition.

3) Two analytical models used in this study, the sway-rocking model and the axi-symmetric FEM model, are confirmed to be valid for evaluating the embedment effects on the soil-structure interaction.

ACKNOWLEDGMENT

This work was carried out by NUPEC as the entrusted project sponsored by the Ministry of International Trade and Industry of Japan. This work was supported by "Sub-committee of Model Tests on Embedment Effect on Reactor Building" under "Committee of Seismic Verification Test" of NUPEC. The authors wish to express their gratitude for the co-operation and valuable suggestions given by the members of the committee.

REFERENCES

Izumi, M. et al., 1990, Model tests on embedment effect on reactor building - Field test (part 8-12): Summaries of Annual Meeting AIJ, Vol.B, 1385-1394 (in Japanese)

Inukai, T. et al., 1991, Experimental study on an embedded soil-structure interaction in a case of hard supporting ground: 2nd International Conference on Recent Advances in Geotechnical Earthquake Engineering and Soil Dynamics, Vol. I, 797-804

Inukai, T. et al., 1991, Forced vibration test on large scale test model on hard rock site (Embedment effect test on soil-structure interaction): SMiRT 11, Vol. K, 135-140

Table 1. Test Results (NS-direction)

TEST	Natural Frequency (Hz)	Damping Ratio (%)	Ratio of Dis. (%)		
			Sway	Rock	Def.
D1	11.0	1.9	9	41	50
D2	11.3	4.4	10	38	52

D1:Non-embedment, D2:Full-embedment
Def.:Deformation of Super-structure

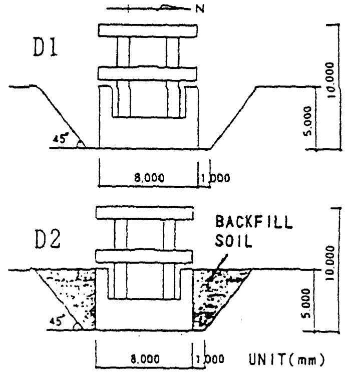

Fig. 1. D-Test Models

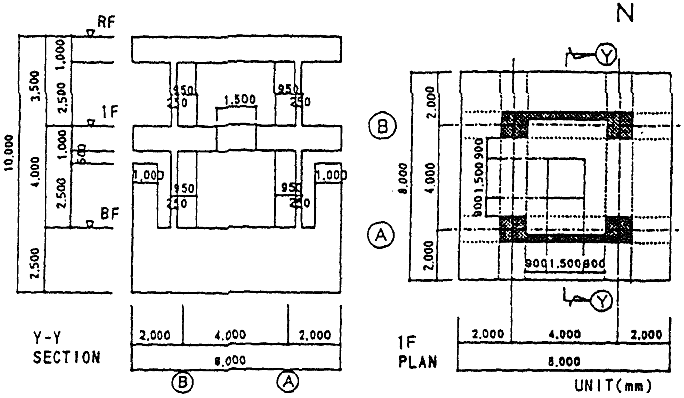

Fig. 2. Shape of Test Model

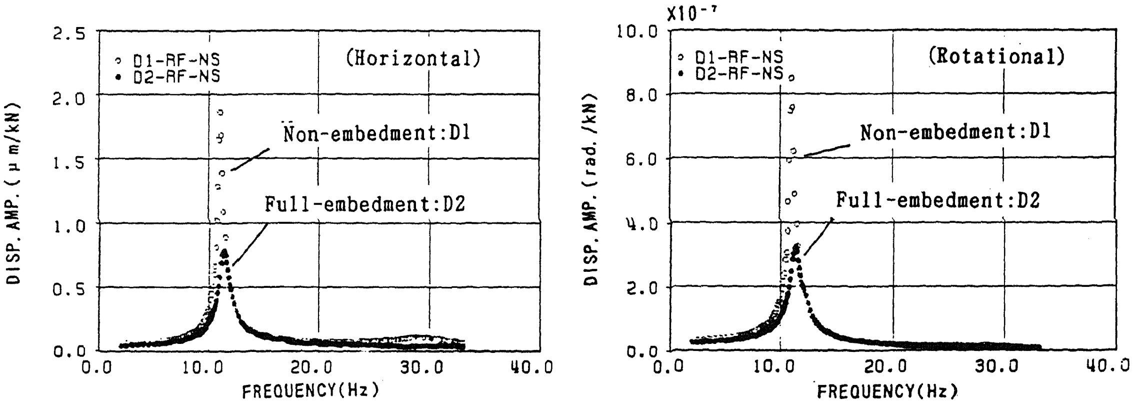

Fig. 3. Resonance Curves of Displacement at Center of Base Bottom

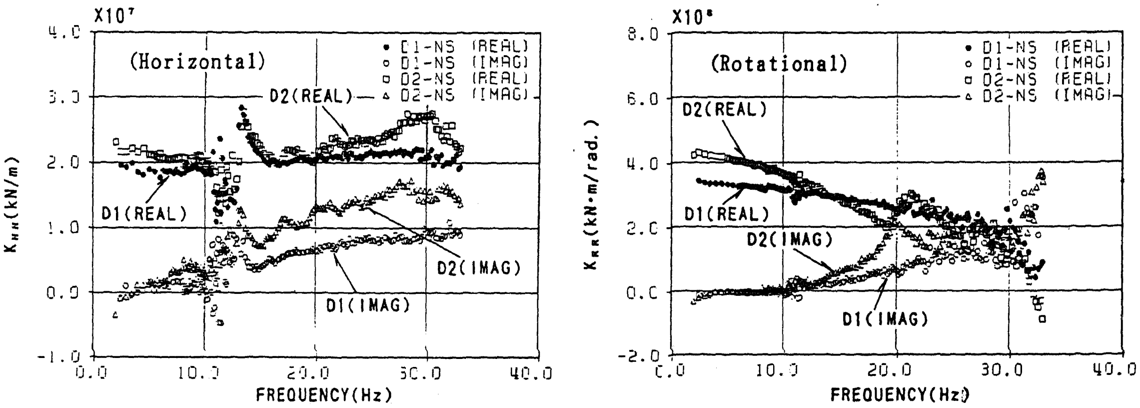

Fig. 4. Dynamic Soil Impedances

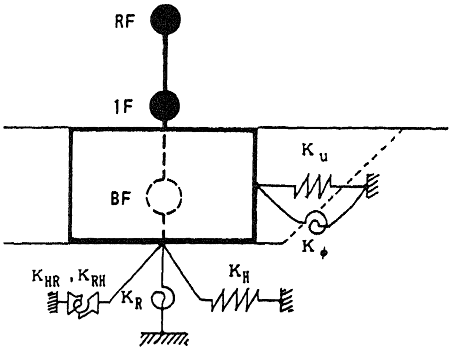

K_H, K_R : Dynamic Horizontal and Rotational Impedances of Base Soil
K_{HR}, K_{RH} : Dynamic Coupling Impedances of Base Soil
K_u, K_ϕ : Dynamic Horizontal and Rotational Impedances of Side Soil

Fig. 5. Sway-Rocking Model

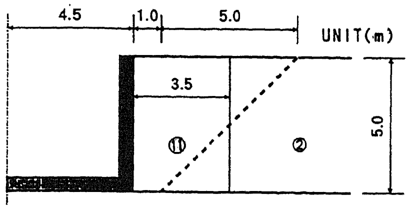

Fig. 6. Analysis Model on Side Impedances by Novak's method

Table 2. Soil Constants

NO	ρ (t/m^3)	V_s (m/s)	E (t/m^2)	ν	h (%)	H (m)
①	1.5	160	11210	0.430	5	2.0
②	1.7	350	60780	0.430	2	3.0
③	1.9	950	447900	0.280	2	5.0
④	1.9	1050	547200	0.280	2	5.0
⑤	1.9	1050	581800	0.361	2	10.0
⑥	1.7	400	71050	0.280	2	0.5
⑦	1.7	110	5460	0.300	4	0.5
⑧	1.7	120	6500	0.300	4	1.0
⑨	1.7	130	7620	0.300	2	1.0
⑩	1.8	140	9360	0.300	2	1.5
⑪	1.8	150	10740	0.300	2	1.0

ρ :Density
E :Young's Modulus
h :Damping Factor
V_s:Shear Wave Velocity
ν :Poisson's Ratio
H :Thickness of Layer

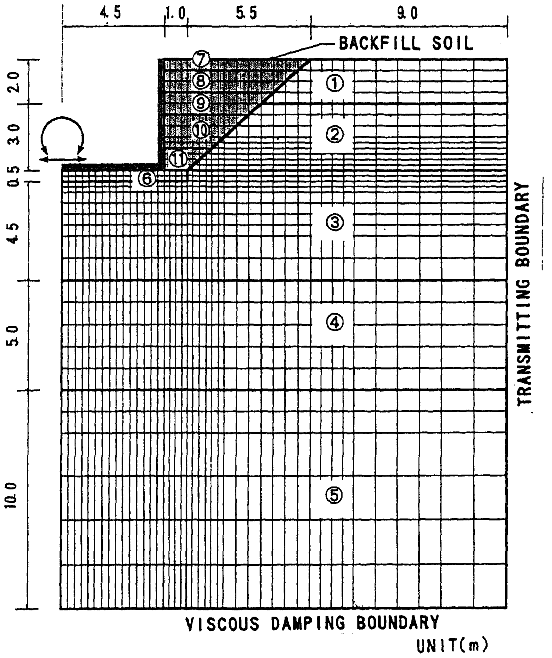

Fig. 7. Axisymmetric FEM Model

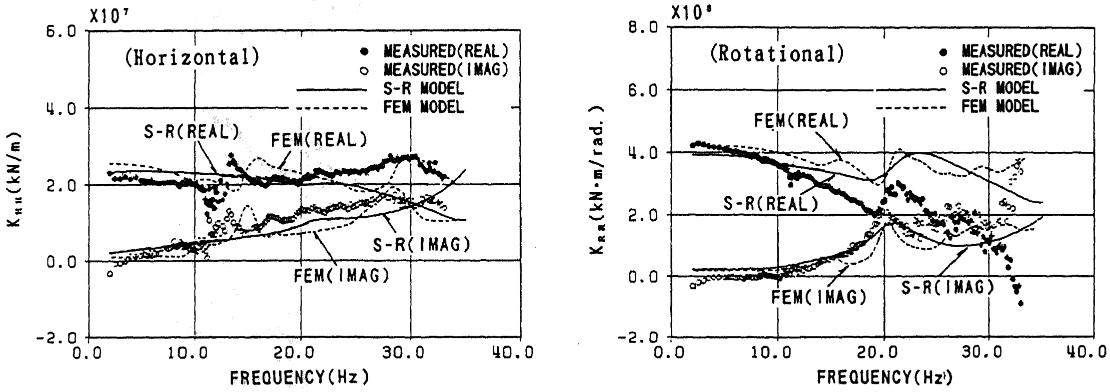

Fig. 8. Comparison of Analyses and Test on Dynamic Soil Impedance (Test D2 : Full-Embedment Case)

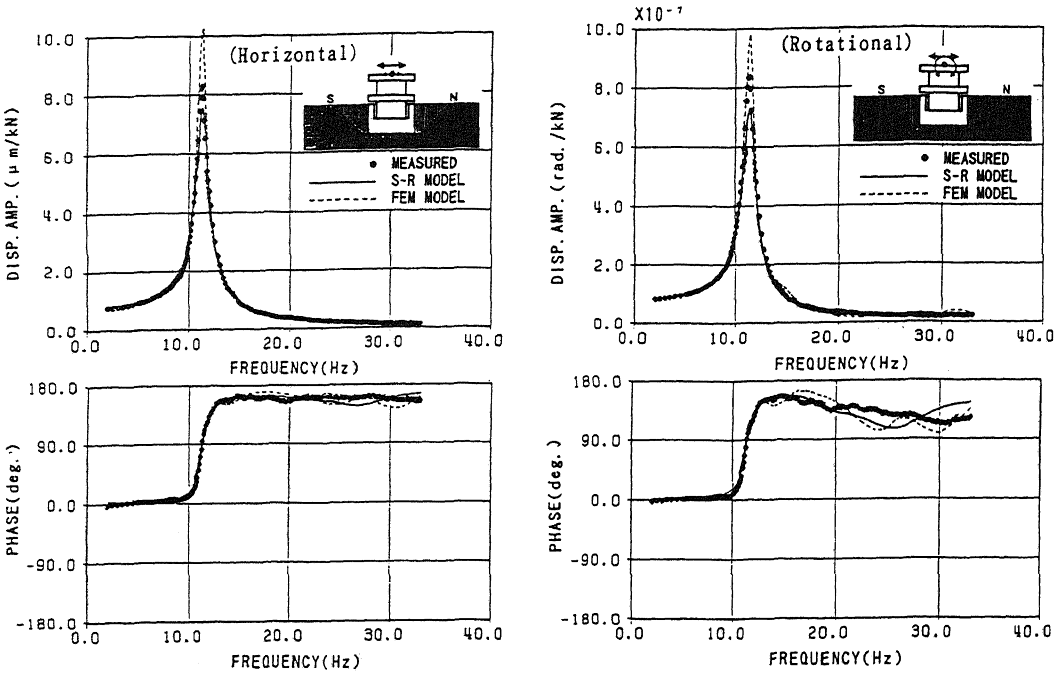

Fig. 9. Comparison of Analyses and Test on Resonance Curve at Top of Test Model (NS-direction Excitation)

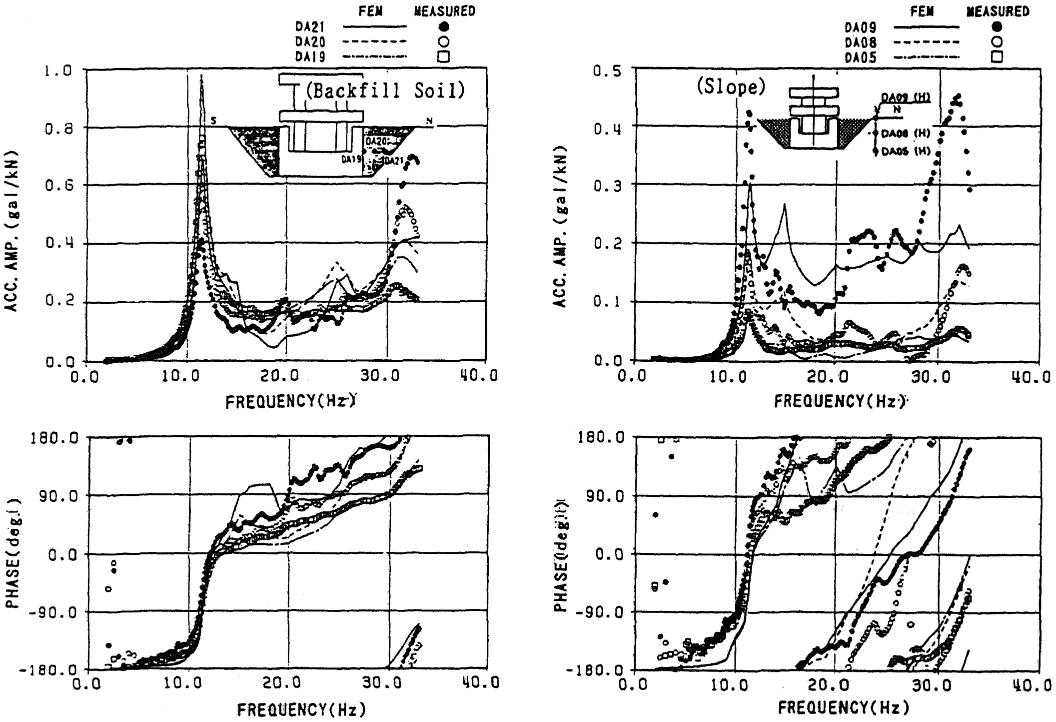

Fig. 10. Comparison of Analysis (FEM) and Test on Resonance Curve in Surrounding Ground (NS-direction Excitation)